THE JOURNAL OF
PHYSICAL CHEMISTRY

VOLUME 84, NUMBER 13 JUNE 26, 1980

Absolute Rate Constant of the Reaction OH + H_2O_2 → HO_2 + H_2O from 245 to 423 K

L. F. Keyser

Jet Propulsion Laboratory, California Institute of Technology, Pasadena, California 91103 *(Received December 10, 1979)*

Publication costs assisted by the National Aeronautics and Space Administration

The absolute rate constant of the reaction between the hydroxyl radical and hydrogen peroxide was measured by using the discharge-flow resonance fluorescence technique at total pressures between 1 and 4 torr. At 298 K the result is $(1.64 \pm 0.32) \times 10^{-12}$ cm^3 molecule^{-1} s^{-1}. The observed rate constant is independent of pressure, surface-to-volume ratio, the addition of vibrational quenchers, and the source of OH. The temperature dependence has also been determined between 245 and 423 K; the resulting Arrhenius expression is k (cm^3 molecule^{-1} s^{-1}) = $(2.51 \pm 0.6) \times 10^{-12} \exp(-126 \pm 76/T)$.

Introduction

The reaction of hydroxyl radical with hydrogen peroxide (eq 1) is important in the HO_x chemistry of the atmosphere. Reaction 1 along with photodissociation (eq 2) and heterogeneous decomposition are considered the major loss processes for hydrogen peroxide in the stratosphere[1-3] and troposphere.[4] Thus, accurate values for the rate coefficient, k_1, especially below 298 K are important in predicting ambient concentrations of hydrogen peroxide by using atmospheric models. Recombination of hydroperoxyl radicals (eq 3) is the major source of atmospheric hydrogen peroxide. Combination of reactions 1 and 3 is equivalent to reaction 4, an important loss of odd hydrogen in the atmosphere. Reactions 1 and 3 provide a parallel path for recombination of OH and HO_2 and can compete with reaction 4, particularly in the lower stratosphere. Reaction 1 also makes a contribution, albeit a minor one, to determining the $[OH]/[HO_2]$ ratio.

$$OH + H_2O_2 \rightarrow HO_2 + H_2O \quad (1)$$

$$H_2O_2 + h\nu \rightarrow OH + OH \quad (2)$$

$$HO_2 + HO_2 \rightarrow H_2O_2 + O_2 \quad (3)$$

$$OH + HO_2 \rightarrow H_2O + O_2 \quad (4)$$

Reaction 1 has been used to generate HO_2 and as a reference in relative rate studies of radical–radical reactions such as reactions 4 and 5.[5,6] An accurate value for k_1 is needed to determine absolute rate constants for these important atmospheric reactions.

$$O + HO_2 \rightarrow OH + O_2 \quad (5)$$

There have been several previous absolute measurements of k_1 at or above room temperature. Harris and Pitts[7] obtained a value of 6.8×10^{-13} cm^3 molecule^{-1} s^{-1} at 298 K by using flash-photolysis resonance fluorescence. Hack et al.[8] used discharge-flow electron spin resonance to determine k_1 between 298 and 666 K. At 298 K they obtained 8.4×10^{-13} cm^3 molecule^{-1} s^{-1}. Greiner[9] studied the reaction between 300 and 458 K by using flash photolysis kinetic spectroscopy; at 300 K the result was 9.5×10^{-13} cm^3 molecule^{-1} s^{-1}. Although the agreement among the studies is relatively good, there are reasons to reexamine the results. For example, at the high initial OH concentrations used by Hack et al., regeneration of OH from the reaction of HO_2 and NO (eq 6) could have interfered with their measurement. The NO was present as a product of the OH formation reaction (eq 7). Secondary reactions may have also interfered with some of the flash-photolysis experiments of Greiner since nonlinear decays of OH were observed at 300 K; in these cases the rate constant was derived from the final slope. One potential problem with

$$HO_2 + NO \rightarrow OH + NO_2 \quad (6)$$

$$H + NO_2 \rightarrow OH + NO \quad (7)$$

0022-3654/80/2084-1659$01.00/0

the Harris and Pitts measurement is their use of flash wavelengths down to 125 nm (CaF_2 window) where H atoms can be generated from H_2O_2 photolysis.[10] Although their results were independent of flash energies from 25 to 100 J, Harris and Pitts did not monitor atomic hydrogen which could interfere by regenerating OH from H_2O_2 and HO_2.

In addition to the absolute measurements described above, two relative rate measurements have been made at room temperature. Meagher and Heicklen[11] obtained $k_1/k_8 = 4.1$ at 298 K from the quantum yield of CO_2 (eq 8) formation during photolysis of H_2O_2, O_2, and CO mix-

$$OH + CO \rightarrow CO_2 + H \quad (8)$$

tures. Gorse and Volman[12] found $k_1/k_8 = 8.13$ at 298 K from the rate of CO_2 production in similar systems. Taking $k_8 = 1.45 \times 10^{-13}$ cm^3 molecule^{-1} s^{-1} [13] yields $k_1 = 5.9 \times 10^{-13}$ and 1.2×10^{-12} cm^3 molecule^{-1} s^{-1}, respectively. This large difference suggests that errors may be present in one or both of the reaction mechanisms used to analyze the data in these relative rate studies.

In the present study, k_1 was determined by using discharge-flow resonance fluorescence from 245 to 423 K. At 298 K the result is $(1.64 \pm 0.32) \times 10^{-12}$ cm^3 molecule^{-1} s^{-1} with only a small temperature dependence over the range studied.

Experimental Section

The apparatus used in these experiments has been described in detail previously.[14,15] Reaction 7 was used to produce OH by adding H atoms to an excess of NO_2. A microwave discharge of approximately 2×10^{-3}% H_2 in helium was used to generate the H atoms. Typical concentrations used were [H] $\leq 10^{11}$ cm^{-3} with [NO_2] = 3×10^{12}–4×10^{12} cm^{-3}. Since reaction 7 can produce vibrationally excited OH up to the $v = 3$ level,[16,17] the NO_2 was added at the upstream end of the constant-temperature region. This allowed approximately 25–50 ms for reaction 7 to go to completion and for vibrational deactivation to occur before the addition of hydrogen peroxide through the movable inlet port. Hydroxyl radicals were detected by resonance fluorescence at a fixed point downstream of the reaction zone. A resonance lamp operated at 40-W microwave power was used to excite the OH fluorescence. A stream of helium which had been saturated with water vapor was passed through the lamp at a total pressure of approximately 2 torr. Hydroxyl radical fluorescence near 308 nm was detected at right angles to the lamp by using an interference filter, photomultiplier tube, and photon counter. The filter used has a maximum transmission of 32% at 310 nm with one-half peak transmission at 306 and 318 nm. Fluorescence signals were calibrated by adding a known amount of NO_2 to an excess of H atoms. Observed signal intensities varied linearly with [OH] up to [OH] = 4×10^{12} cm^{-3}. At [OH] = 1×10^{11} cm^{-3}, the signal intensity was about 10^4 s^{-1} with scattered light less than 900 s^{-1}. Thus, for a 10-s counting time, the minimum detectable [OH] (S/N = 1.5) was approximately 2×10^8 cm^{-3}. Experimental runs were carried out for the most part with [OH] between 10^9 and 10^{11} cm^{-3}. The scattered-light signal was determined by using two methods: (1) the discharge producing atomic hydrogen was turned off while maintaining all flows at the same level and (2) with the atomic hydrogen discharge on, the NO_2 was turned off, and a large excess of propylene was added to remove any residual OH. Scattered-light levels with method 2 generally were a few percent higher, but there was no significant difference in the rate constants obtained by using either method.

Hydrogen peroxide was added in a stream of helium through a movable inlet jet. High flow rates were used to minimize decomposition, and surfaces in contact with hydrogen peroxide were quartz, Pyrex, or Teflon only. Below 298 K hydrogen peroxide was found to condense in the movable inlet tube before expansion into the low-pressure flow-tube reactor. Condensation was prevented by use of a jacketed inlet tube maintained near 30 °C along its entire length by circulating methanol from an external bath. Hydrogen peroxide concentrations were determined photometrically at 199.5 nm immediately upstream of the inlet. An absorption cross section of 4.8×10^{-19} cm^2 (base e) was used. This was determined previously with the absorption cell and optical train used in these experiments.[15] Concentrations of hydrogen peroxide in the reactor tube were controlled by varying the absorption-cell pressure at a fixed helium flow of about 0.45 L atm min^{-1} (at 293 K). Hydrogen peroxide pressures in the cell were approximately 1.2 torr with total pressures between 45 and 500 torr. Flow velocities in the 2.4-cm diameter by 25 cm absorption cell were between 2.5 and 30 cm s^{-1}.

The reactor tube was provided with glass flanges (sealed with Viton O rings) at each end to facilitate change of wall coatings and tube sizes. To reduce OH wall losses, the reactor was coated with either phosphoric acid or a halocarbon wax (Series 15-00, obtained from Halocarbon Corp., Hackensack, NJ). Tube diameters used were 12.6, 25.0, and 50.6 mm. Total helium carrier gas flow rates were 0.8–2.7 L atm min^{-1} (at 293 K) with pressures between 1 and 4 torr. Flow velocities were 1000–2000 cm s^{-1}.

The wall loss of OH was measured by adding NO_2 through the movable inlet. Both excess H atoms and excess NO_2 were used. The resulting k_w was less than 10 s^{-1} on both wax-coated and baked phosphoric acid coated walls. No large change in k_w was observed when it was measured immediately after exposing the walls to hydrogen peroxide.

Gases used were chromatographic grade helium (99.9999%), research grade hydrogen (99.9995%), nitric oxide, CP (99.0%), sulfur hexafluoride (99.8%), oxygen UHP (99.99%), carbon dioxide Coleman grade (99.99%), 5% fluorine in helium, and nitrogen dioxide (99.5%). The nitrogen dioxide was purified by adding excess oxygen in the gas phase. After several hours, the oxygen was removed by slowly passing the mixture through a −78 °C trap. The resulting white solid showed no indication of the blue coloration due to nitric oxide impurities. The nitrogen dioxide was stored at −196 °C and distilled to a −78 °C trap before use. In some cases the nitrogen dioxide was prepared by reacting nitric oxide with a large excess of oxygen. Hydrogen peroxide (90%) was obtained from FMC and was concentrated to approximately 95% by pumping.

Results and Discussion

To minimize secondary reactions, pseudo-first-order conditions were used with hydrogen peroxide in large excess over OH. Generally, initial concentrations of OH were less than 10^{11} cm^{-3} with hydrogen peroxide between 2×10^{13} and 18×10^{13} cm^{-3}. Under these conditions

$$\ln (I_0/I) = k_1' l/\bar{v} \quad (9)$$

where I and I_0 are respectively the OH fluorescence signal with and without added hydrogen peroxide, k_1' is the pseudo-first-order rate constant, l is the reaction length, and $\bar{v}$ is the average flow velocity. Plots of $\ln (I_0/I)$ vs. l generally were linear over two reaction lifetimes or more. However, some plots showed negative curvature (lower slopes) at long reaction times. This may be due to re-

TABLE I: Rate Constants for the OH + H_2O_2 Reaction

temp, K	press., torr	flow-tube diam, mm	runs	$10^{12}k_1$,[a] cm³ molecule⁻¹ s⁻¹ av[b]	slope[c]	intercept[c]
298	1	50.6[d]	14	1.80 ± 0.14	1.67 ± 0.07	8 ± 5
298	1	50.6[e]	9	1.74 ± 0.16	1.54 ± 0.11	16 ± 10
298	2-4	25.0[d]	38	1.75 ± 0.22	1.45 ± 0.16	26 ± 14
298	4	12.6[d]	9	1.59 ± 0.32	1.64 ± 0.48	−4 ± 48
298	2-4	25.0[f]	22	2.16 ± 0.28	1.88 ± 0.17	24 ± 17
overall av at 298 K				1.81 ± 0.42	1.64 ± 0.32	
423	1.5	50.6[d]	7	2.12 ± 0.16	1.92 ± 0.08	14 ± 7
371	1	50.6[d]	7	1.96 ± 0.20	1.76 ± 0.14	16 ± 14
335	1	50.6[d]	8	1.86 ± 0.20	1.63 ± 0.05	20 ± 5
273	1	50.6[d]	8	1.87 ± 0.14	1.71 ± 0.10	12 ± 10
245	1	50.6[d]	8	1.81 ± 0.17	1.45 ± 0.07	28 ± 6

[a] Errors are ± 2σ. [b] From average of individual $k_1'/[H_2O_2]$ values. [c] From plot of k_1' vs. $[H_2O_2]$. [d] Coated with halocarbon wax, H + NO_2 to produce OH. [e] Coated with halocarbon wax, F + H_2O to produce OH. [f] Coated with phosphoric acid, H + NO_2 to produce OH.

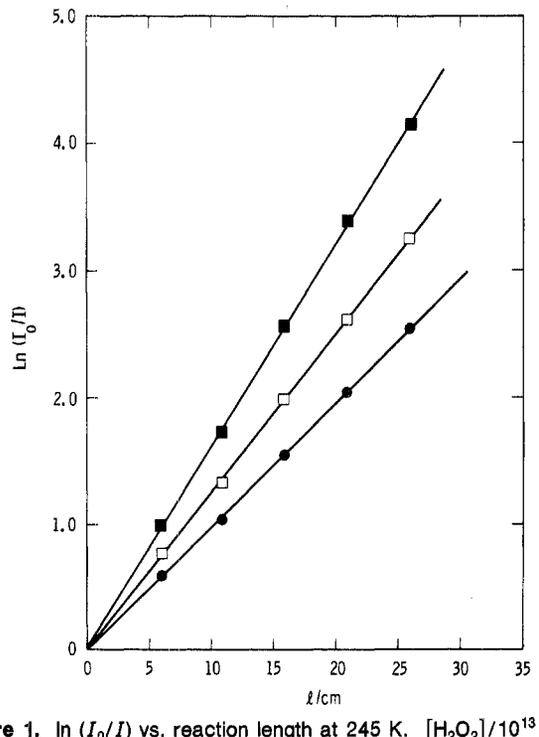

Figure 1. ln (I_0/I) vs. reaction length at 245 K. $[H_2O_2]/10^{13}$ cm^{-3} and ($\bar{\nu}$/cm s^{-1}) as follows: ■, 12.6 (1325); □, 9.14 (1305); ●, 6.73 (1290). Lines are linear least-squares fits.

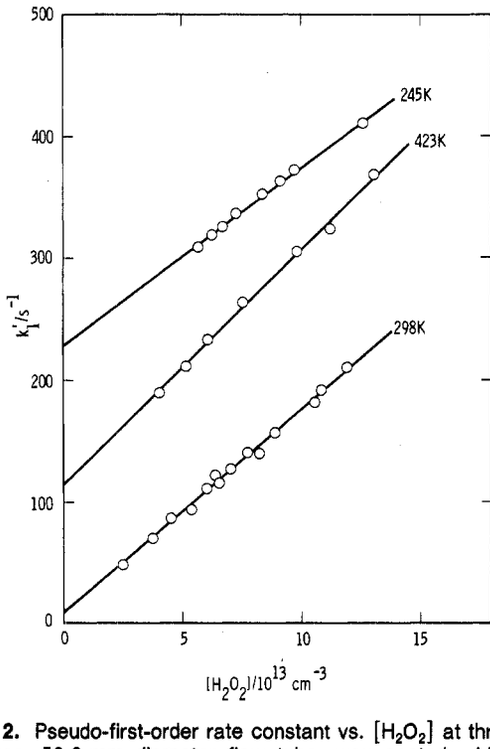

Figure 2. Pseudo-first-order rate constant vs. $[H_2O_2]$ at three temperatures, 50.6-mm diameter flow tube, wax coated. Lines are least-squares fits of the experimental points. For clarity, the 423 and 245 K data have been displaced by 100 and 200 s^{-1}, respectively.

generation of OH from the reaction of product HO_2 with NO formed by reaction 7. When curvature was observed, the initial slope was used to calculate k_1'. Plots of ln (I_0/I) vs. l at 245 K are shown in Figure 1. The lines through the points are linear least-squares fits of the data. The bimolecular rate constant, k_1, was determined from the slope of k_1' vs. $[H_2O_2]$ plots and from an average of individual $k_1'/[H_2O_2]$ values. Typical k_1' vs. $[H_2O_2]$ plots are shown in Figure 2. The rate data are summarized in Table I and plotted in Arrhenius form in Figure 3. The resulting Arrhenius expression is

$$k_1 \text{ (cm}^3 \text{ molecule}^{-1} \text{ s}^{-1}) = (2.51 \pm 0.62) \times 10^{-12} \exp[(-126 \pm 76)/T] \quad (10)$$

$$245 \leq T \leq 423 \text{ K}$$

Corrections have been made for axial diffusion and for the viscous pressure drop between the reaction zone and the pressure measurement port located downstream.[18] Diffusion coefficients for the hydroxyl radical in helium were estimated by using experimental values for atomic oxygen in helium and neon in helium.[19] The values used were 1.75 atm cm^2 s^{-1} at 423 K, 1.40 at 371 K, 1.18 at 335 K, 0.97 at 298 K, 0.83 at 273 K, and 0.69 at 245 K. Pressure corrections to k_1 were generally in the range 2–8% whereas axial diffusion corrections were less than 6%. No corrections were made for radial diffusion since estimates indicate that it is small under the conditions used. The error limits given in Table I and eq 10 are twice the standard deviation obtained from the data analysis. Overall experimental uncertainty including errors in the hydrogen peroxide determination is estimated at ±20–25%.

Surface Reactions. The pseudo-first-order rate constant, k_1', obtained from ln (I_0/I) vs. l plots may be equated to the product of the true bimolecular rate constant and the hydrogen peroxide concentration ($k_1' = k_1[H_2O_2]$) as long as the first-order wall loss of OH is independent of the presence or absence of hydrogen peroxide[20] and no bimolecular surface reaction between OH and hydrogen peroxide contributes. In general

$$k_1'(\text{obsd}) = k_1[H_2O_2] + k_{1\,\text{wall}}[H_2O_2] + \Delta k_{\text{wall}} \quad (11)$$

where k_1 is the gas-phase bimolecular rate constant, $k_{1\,\text{wall}}$ is the bimolecular rate constant for a possible heteroge-

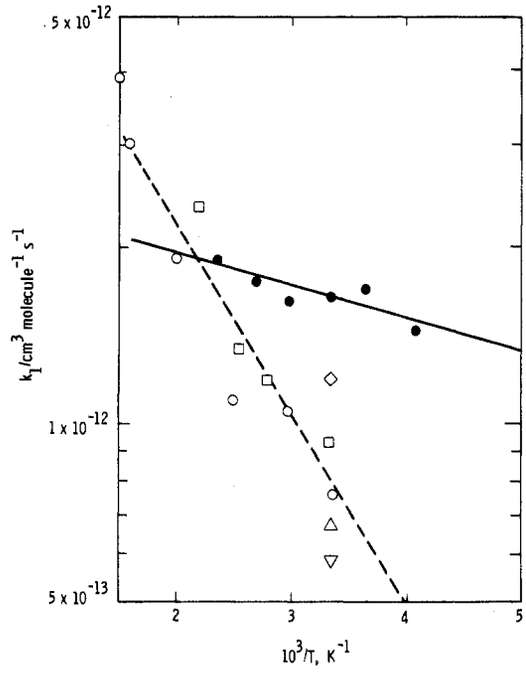

Figure 3. Comparison of present results with earlier measurements of k_1. The symbols are as follows: ●, this work; △, Harris and Pitts, ref 7; ○, Hack et al., ref 8; □, Greiner, ref 9; ▽, Meagher and Heicklen, ref 11; ◇, Gorse and Volman, ref 12. The dashed line represents the Arrhenius expression previously used in atmospheric models, based on ref 8 and 9. The solid line is a least-squares fit of the present data alone.

TABLE II: Effect of Added Vibrational Quenchers

quencher	quenching rate constant, 10^{-13} cm^3 molecule^{-1} s^{-1}	concn range, 10^{15} cm^{-3}	a
O_2	0.1-7.8[b]	5-12	1.0 ± 0.1
SF_6		10	1.0 ± 0.06
H_2O	2-135[c]	7.3-8.8	1.1 ± 0.1
CO_2	0.25[d]	7.8-10	0.9 ± 0.1

[a] k_1(298 K, with quencher)/k_1(298 K, without quencher). [b] References 21, 22, and 23. [c] References 23 and 24. [d] References 21 and 23.

neous reaction between OH and hydrogen peroxide, and Δk_{wall} is the change in the first-order wall loss of OH when hydrogen peroxide is added. Most of the k_1' vs. $[H_2O_2]$ plots show small positive intercepts which appear to be significant since they are greater than twice the standard deviation from the origin. This implies that when hydrogen peroxide is added, the first-order OH wall loss increases because of hydrogen peroxide itself, water vapor which is added with the H_2O_2, or possibly a product of the reaction. Because of the positive intercepts, the slopes of the k_1' vs. $[H_2O_2]$ plots should give better estimates of k_1 than the averages, and the slopes are used in the remainder of this discussion. It should be noted that the differences in k_1 using averages or slopes are less than 25%.

Contributions to the observed rate constant from a wall loss of hydroxyl radical which is proportional to $[H_2O_2]$ (second term on right-hand side of eq 11) cannot be eliminated by use of the slope in k_1' vs. $[H_2O_2]$ plots. To check for this possibility, the surface-to-volume ratio and the wall coating were changed at 298 K. The experiments were carried out under conditions where radial diffusion is rapid so that the wall rate constant is proportional to the surface condition and the surface-to-volume ratio.[18] With a phosphoric acid coating, the observed rate constant was about 30% higher than with a halocarbon wax coating (compare row five with the first four rows of Table I). This is just outside the estimated experimental uncertainty and may indicate a small surface effect. However, when the surface-to-volume ratio was varied over a factor of 4 in wax-coated tubes, no significant change in the rate constant was observed (first four rows of Table I). These results imply that there is little or no contribution to the observed rate from a second-order surface reaction.

Secondary Reactions. At the high stoichiometric ratios used ($[H_2O_2]/[OH]_0 \geq 200$, with $[OH]_0 \leq 10^{11}$ cm^{-3}) estimates indicate that secondary reactions such as 4, 6, 12, and 13 should not interfere with the present measure-

$$OH + OH \rightarrow H_2O + O \quad (12)$$

$$O + OH \rightarrow O_2 + H \quad (13)$$

ments. As a check, the initial [OH] was varied from 0.41 × 10^{11} to 6.6 × 10^{11} cm^{-3} at a constant hydrogen peroxide concentration of 9.6 × 10^{13} cm^{-3}. No significant change was observed in k_1, indicating that secondary reactions are not important.

Vibrationally Excited OH. Because of the long delay times (45–70 ms) between OH formation and detection, vibrationally excited OH from reaction 7 should not contribute significantly to the observed fluorescence signal and, thus, should not interfere directly with the present measurements. To test for possible effects of vibrational excitation on the observed rate constant, we added a series of quenchers to the reaction mixture with $[OH]_0 \leq 10^{11}$ cm^{-3} and $6 \times 10^{13} \leq [H_2O_2] \leq 15 \times 10^{13}$ cm^{-3}. Five or six runs were carried out with each quencher. The results are summarized in Table II. In the presence of high concentrations of vibrational quenchers, k_1 observed agrees with the values obtained without added quenchers to within ±10%, which is well within expected experimental error.

As an additional check on possible interference from vibrational excitation, the reaction of atomic fluorine with water was used in place of reaction 7 to generate OH (eq 14). At 298 K, $k_{14} = 1.1 \times 10^{-11}$ cm^3 molecule^{-1} s^{-1}.[13b]

$$F + H_2O \rightarrow OH + HF \quad (14)$$

Observation of infrared chemiluminescence from product HF but not from OH is evidence that reaction 14 produces OH predominantly in the ground vibrational level.[25] In the present experiments fluorine atoms were generated in a microwave discharge of approximately 2×10^{-3}% F_2 in helium and reacted with an excess of water. A series of nine runs at 298 K and 1 torr were carried out with $4.5 \times 10^{13} \leq [H_2O_2] \leq 15 \times 10^{13}$ cm^{-3}, $0.9 \times 10^{11} \leq [F_2]_0 \leq 1.3 \times 10^{11}$ cm^{-3} and $[H_2O] = 2.9 \times 10^{14}$ cm^{-3}. The results are summarized in row 2 of Table I and are not significantly different from those obtained by using reaction 7 as the source of OH. These results and the results with added quenchers show that vibrationally excited OH does not interfere with the present measurements.

Hydrogen Peroxide Determination. As discussed in the Experimental Section, hydrogen peroxide was measured photometrically by using an absorption cross section which was redetermined on the present apparatus. The value used is in excellent agreement with recent measurements using two analytical methods.[26,27] As an additional check on the determination, hydrogen peroxide was sampled downstream of the reaction zone by trapping at −196 °C. Analyses agreed within 5% with the upstream photometric measurements.

Relative Rate Measurements. As an additional test for possible contributions from interfering reactions, the rate of reaction 1 was measured relative to the well-known rate constant for reaction 6. Experimental conditions were adjusted to allow the concentrations of both OH and HO_2

TABLE III: Summary of Relative Rate Measurements, k_1/k_6

$\bar{v}$, cm s^{-1}	$[HO_2]_{ss}/[OH]_{ss}$	$10^{-14} \times [H_2O_2]$, cm^{-3}	$10^{-13} \times [NO]$, cm^{-3}	k_1/k_6
1570	0.978	1.11	2.03	0.179
980	0.990	1.12	2.11	0.186
980	1.120	1.73	2.90	0.188
980	1.107	2.35	3.92	0.185
			av	0.184 ± 0.05[a]

[a] Error includes estimate of overall experimental uncertainty.

to come to an approximate steady state. HO_2 was determined after converting it to OH by adding a large excess of NO (2.7×10^{14} cm^{-3}) a few milliseconds upstream of the fluorescence cell. Three to five determinations were made during each of four runs at 298 K and 1 torr by using $[OH]_0 \leq 10^{11}$ cm^{-3}, $1.0 \times 10^{14} \leq [H_2O_2] \leq 2.4 \times 10^{14}$ cm^{-3} and $2.0 \times 10^{13} \leq [NO] \leq 3.9 \times 10^{13}$ cm^{-3}. Under these conditions losses of OH and HO_2 by reaction 4 or wall reactions ($k_w < 10$ s^{-1}) are negligible compared to reactions 1 and 6 and

$$k_1/k_6 = [HO_2][NO]/[OH][H_2O_2] \quad (15)$$

The results are summarized in Table III. Small corrections less than 7% have been made for the reduction in the OH fluorescence signal following addition of the excess NO. This reduction may be due to increased OH wall loss in the presence of NO. Corrections of 7–15% have also been made for incomplete conversion of HO_2 to OH. Using the observed ratio of 0.184 ± 0.05 and a value of (8.0 ± 1.0) $\times 10^{-12}$ for k_6[28] yields a value of (1.5 ± 0.6) $\times 10^{-12}$ cm^3 $molecule^{-1}$ s^{-1} for k_1, which is in good agreement with the absolute measurement. Owing to the limited number of runs, these relative rate measurements should not be considered as a separate determination of k_1. They do serve, however, as a check on the consistency of the present measurements with the accepted value for k_6.

The present results are compared with earlier measurements of k_1 in Figure 3. Except for the results of Gorse and Volman, the earlier measurements of k_1 are approximately a factor of 2 lower than the present value at 298 K. This large difference is outside the expected combined experimental errors of these measurements and indicates that unrecognized complications may be present in some of the studies. As discussed above, interferences from secondary reactions, errors in the hydrogen peroxide determination, surface reactions, or excited-state reactions were found not to be important in the present experimental approach. Possible reasons for the difference between the present results and the earlier absolute measurements of Hack et al., Greiner, and Harris and Pitts have been discussed above.

Burrows et al.[5] used reaction 1 as a reference in relative rate measurements of several HO_2 reactions. For k_6/k_1, they report 10.3 ± 3.0. The present result of 5.4 ± 1.5 for this ratio is just outside the estimated error limits of the two measurements. The central value of the present ratio measurement and the present absolute determination of k_1 are consistent with the accepted value for k_6 of (8 ± 1) $\times 10^{-12}$ cm^3 $molecule^{-1}$ s^{-1}.[28] The central value of Burrows et al.'s ratio measurement is completely inconsistent with the present results and the accepted value for k_6. The reason for this difference in the ratio measurements is not clear at this time.

The present determination of k_1 can have a substantial effect on predicted hydrogen peroxide concentrations in the atmosphere. Table IV compares the loss of H_2O_2 due to reaction 1 with photodissociation at altitudes from 10–50 km. Use of the present value for k_1 increases the loss rate by a factor of 2.5 at 50 km and 4.5 at 20 km. Loss of H_2O_2 due to reaction 1 competes with photodissociation over most of the stratosphere.

TABLE IV: Loss of H_2O_2 in the Atmosphere

altitude, km	T,[a] K	$10^{-6} \times [OH]$,[b] cm^{-3}	$10^7 k_1[OH]$, s^{-1} previous value[c]	$10^7 k_1[OH]$, s^{-1} this work	$10^7 J_{2}$,[d] s^{-1}
10	223	1.6	5.5	23	72
20	217	0.58	1.8	8.2	87
30	227	3.3	12	48	160
40	250	28	140	430	480
50	271	22	140	350	960

[a] Standard atmosphere, 45° latitude. [b] Average annual daytime values, ref 2. [c] Calculated by using $k_1 = 1 \times 10^{-11} \exp(-750/T)$, ref 13a. [d] Solar zenith angle = 0°, ref 26.

While this manuscript was in preparation, the author learned of a similar study by Sridharan et al.[29] Their results are in excellent agreement with the present measurement of k_1.

Acknowledgment. The author thanks W. B. DeMore and C. J. Howard for valuable discussions in the course of this work. The research described in this paper was carried out at the Jet Propulsion Laboratory, California Institute of Technology, under NASA Contract NAS7-100.

References and Notes

(1) M. Nicolet, *Aeron. Acta A*, **No. 156** (1975).
(2) P. J. Crutzen, I. S. A. Isaksen, and J. R. McAfee, *J. Geophys. Res.*, **83**, 345 (1978).
(3) S. C. Wofsy, *J. Geophys. Res.*, **83**, 364 (1978).
(4) H. Levy, II, *Adv. Photochem.*, **9**, 369 (1974).
(5) (a) J. P. Burrows, G. W. Harris, and B. A. Thrush, *Nature (London)*, **267**, 233 (1977); (b) J. P. Burrows, D. I. Cliff, G. W. Harris, B. A. Thrush, and J. P. T. Wilkinson, *Proc. R. Soc. London*, in press.
(6) W. Hack, A. W. Preuss, and H. Gg. Wagner, *Ber. Bunsenges. Phys. Chem.*, **82**, 1167 (1978).
(7) G. W. Harris and J. N. Pitts, Jr., *J. Chem. Phys.*, **70**, 2581 (1979).
(8) W. Hack, K. Hoyermann, and H. Gg. Wagner, *Int. J. Chem. Kinet., Symp.*, **1**, 329 (1975).
(9) N. R. Greiner, *J. Phys. Chem.*, **72**, 406 (1968).
(10) R. B. Klemm, W. A. Payne, and L. J. Stief, *Int. J. Chem. Kinet., Symp.*, **1**, 61 (1975).
(11) J. F. Meagher and J. Heicklen, *J. Photochem.*, **3**, 455 (1975).
(12) R. A. Gorse and D. H. Volman, *J. Photochem.*, **1**, 1 (1972).
(13) (a) R. D. Hudson, Ed., *NASA Ref. Publ.*, **No. 1010** (1977); (b) D. L. Baulch, R. A. Cox, R. F. Hampson, Jr., J. A. Kerr, J. Troe, and R. T. Watson, CODATA Task Group on Chemical Kinetics, *J. Phys. Chem. Ref. Data*, in press.
(14) L. F. Keyser, *J. Chem. Phys.*, **69**, 214 (1978).
(15) L. F. Keyser, *J. Phys. Chem.*, **84**, 11 (1980).
(16) J. C. Polanyi and J. J. Sloan, *Int. J. Chem. Kinet., Symp.*, **1**, 51 (1975).
(17) J. H. Brophy, J. A. Silver, and J. L. Kinsey, *J. Chem. Phys.*, **62**, 3820 (1975).
(18) F. Kaufman, *Prog. React. Kinet.*, **1**, 1 (1961).
(19) T. R. Marrero and E. A. Mason, *J. Phys. Chem. Ref. Data*, **1**, 3 (1972).
(20) A. A. Westenberg and N. deHaas, *J. Chem. Phys.*, **46**, 490 (1967).
(21) T. E. Kleindienst and B. J. Finlayson-Pitts, Abstracts of Pacific Conference on Chemistry and Spectroscopy, Pasadena, CA, Oct 1979.
(22) G. E. Streit and H. S. Johnston, *J. Chem. Phys.*, **64**, 95 (1976).
(23) S. D. Worley, R. N. Coltharp, and A. E. Potter, Jr., *J. Phys. Chem.*, **76**, 1511 (1972).
(24) J. E. Spencer and G. P. Glass, *Int. J. Chem. Kinet.*, **11**, 97 (1977).
(25) H. W. Chang, D. W. Setser, M. J. Perona, and R. L. Johnson, *Chem. Phys. Lett.*, **9**, 587 (1971).
(26) C. L. Lin, N. K. Rohatgi, and W. B. DeMore, *Geophys. Res. Lett.*, **5**, 113 (1978).
(27) L. T. Molina, S. D. Schinke, and M. J. Molina, *Geophys. Res. Lett.*, **4**, 580 (1977).
(28) C. J. Howard, *J. Chem. Phys.*, **71**, 2352 (1979), and earlier references cited therein.
(29) U. C. Sridharan, B. Reimann, and F. Kaufman, *J. Chem. Phys.*, in press.